AEROELASTIC TAILORING OF A CIVIL TILTROTOR CONFIGURATION

Martin Stettner
Graduate Research Assistant

Dimitri N. Mavris
Manager

Daniel P. Schrage
Director

Aerospace Systems Design Laboratory
Georgia Institute of Technology
Atlanta, Georgia 30332

ABSTRACT

Progress in establishing an analysis package and design/optimization framework for preliminary design of a civil tiltrotor aircraft is reported. Updates to the sizing/performance program VASCOMP and Equivalent LAminated Plate Solution ELAPS are described. Correlation of this updated ELAPS (now including shear panels) and a state-space unsteady aerodynamic analysis, PWAKE, with reference results from the Automated STRuctural Optimization System, ASTROS, is shown. A generic UNIX-based, flexible executive system for multidisciplinary design/ optimization tasks is presented. The framework features a central data base, provisions for parallel analysis execution on different host computers connected to the same file server, local sensitivity calculation using finite differencing, global sensitivity calculation using the Global Sensitivity Equation (GSE), and a utility allowing different levels of user control. A simple sample case demonstrates proper framework operation and practical advantages in accuracy in the GSE approach versus global finite differencing.

INTRODUCTION

Civil Tiltrotor (CTR) Aircraft have recently been considered as a means for alleviation of aircraft congestion problems. A series of research efforts, as collected in the Boeing CTR study [1] have supported the CTR's potential to be an economically viable and technically feasible solution in the short to medium range sector. However, this market segment is highly competitive and saturated by a large variety of mature turboprop aircraft designs. The CTR's main disadvantage can be formulated in terms of Sobieski's "what if" question [2]: How does a local design change affect the rest of the design? There is a substantial data base for turboprop aircraft, which can be used to answer this question for a large number of problems. One example is statistical wing weight trend equations. The tiltrotor aircraft (TR) is a much more complex system, mainly due to rotor - related phenomena like proprotor whirl flutter [3], and there are only a limited number of existing designs. As a result, the "what if" question must be answered by modeling the configuration from the start of the design process. Since coupling between disciplines at this stage must at least be anticipated, modeling should be as complete as possible. This not only includes the TR's aeroelastic phenomena but also performance and economics models: The prime goal is not simply technical feasibility, but economic competitiveness.

Previous TR design studies have focused either on performance trends in sizing using low-fidelity representations of aeroelastic design constraints, or on technical approaches to whirl flutter alleviation. Two recent examples illustrate these branches: Schleicher [4] wrapped a numerical optimization loop around the V/STOL aircraft sizing and performance program VASCOMP [5], which incorporates a simplistic wing design based on frequency placement, and Nixon [6] performed extensive trend studies on the effect of uncoupled rotor and wing natural frequencies on whirl flutter. The necessity of including aeroelastic constraints in economics-driven tiltrotor aircraft design has been established in Reference [7], so these two areas must be combined. Reference [8] suggested a comprehensive, modular approach to CTR optimization using separate analysis tools for mission performance/sizing (VASCOMP), wing structure (ELAPS [9]), wing unsteady aerodynamics, rotor aeroelasticity and rotor/wing coupling (PASTA [3]), and control system design. According to the proposed scheme, integration of these contributing analyses is provided by a flexible design environment which utilizes utilities of the UNIX operating system. This report summarizes previously presented and recently obtained results in the two focus areas of this research:

Presented at the American Helicopter Society Vertical Lift Aircraft Design Conference, San Francisco, California, January 18-20, 1995.

(a) selection, improvement, or development and calibration of existing or new analytical tools for CTR modeling;

(b) development of a flexible, portable, generic design and optimization framework.

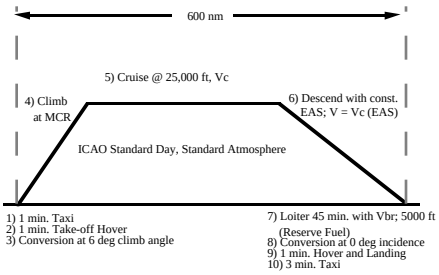

Fig. 1: Design Mission Profile

ANALYTICAL MODELS

The selection of tools for the Contributing Analyses (CAs) mentioned above was governed by the goal of achieving a "homogeneous complexity" approach, i.e. focusing on one or more disciplines by using more sophisticated tools was to be avoided. This required modifications to some of the existing tools and development of a new unsteady aerodynamics code, as described in the following sections.

Sizing and Mission Performance

VASCOMP sizes the CTR aircraft for a given mission (Fig. 1, described in [7]) and general layout. As a result, it provides geometry information for the other analyses and mission performance data which can be used to calculate a system level optimization objective function. In this particular application, a simplified indicator for aircraft performance to cost ratio, the Productivity Index,

$$PI = \frac{\text{Payload} * \text{Block Speed}}{\text{Empty Weight} + \text{Fuel Weight}}$$

is used. For coupling with the other CAs, the sizing task is more important. In addition to the obvious necessity for providing the aircraft's physical dimensions, the component weights and locations are crucial for the aeroelastic stability analysis. For a cantilevered wing, Friehmelt [10] notes the sensitivity of whirl flutter speed to the chordwise nacelle center of gravity location. Equivalently, the nacelle mass is major driver for the wing internal design, and special care must be taken in obtaining weights of components located in the nacelle. When experimenting with VASCOMP Version 1.09, some runs with the Variable Diameter Tiltrotor (VDTR) option indicated that engine and transmission were sized for the conversion condition. A close investigation of this option revealed that the rotor diameter was equal to the hover diameter through the entire conversion segment. Reduction of the rotor diameter decreased the peak transmission torque and resulted in significant weight savings. As a result, the code was extended to include diameter scheduling: Between 0˚ and 60˚ conversion angle, the rotor diameter increases linearly from cruise to hover diameter, and is constant above 60˚. This profile resembles the schedule for constant tip-fuselage distance from Fig. 2 of Reference [11], but is otherwise an arbitrary choice. The same is the case for the acceleration profile during conversion (acceleration as a function of velocity). The profile used by Nixon (Fig. 4 in Reference [6]) with a constant peak acceleration of 0.2g between 1/3 and 2/3 of the conversion speed is used unchanged. Both the diameter schedule and the conversion acceleration are expected to have significant impact on the transmission size, but are omitted for the sake of simplicity.

Rotor performance for constant diameter cases is calculated using existing Figure of Merit and propulsive efficiency tables used by Nixon [6]. New tables were created for VDTR cases by curve-fitting experimental data obtained by Studebaker and Matuska [11].

Wing Structure

ELAPS has been chosen for static and dynamic analysis of the wing structure, since in Reference [9] excellent correlation with results from the EAL finite element analysis [12] was shown, while utilizing much less degrees of freedom and thus reducing computational effort. However, ELAPS assumes Kirchhoff's kinematic assumptions of classical plate theory. If the structure is soft in transverse shear, the equivalent plate model is too stiff, since it does not allow this degree of freedom (an extensive comparison of classical equivalent plate models such as ELAPS, extended models which include transverse shear, and finite element models for HSCT wings which are soft and stiff in transverse shear can be found in Reference [13]). Modelling typical tiltrotor wing boxes without transverse shear deformation is expected to be non-conservative. These structures have only two spars and a depth:chord:semi-span ratio of roughly 0.5:1.0:6.0. Hence, shear effects are important, particularly since torsional stiffness of the wing is critical for whirl flutter. Since ELAPS tiltrotor wing

models exist and significant experience with the code has been accumulated in previous studies at the Aerospace Systems Design Laboratory [10], ELAPS was modified to include the new degree of freedom.

In the original ELAPS, the structural deflections are represented by power series in the normalized spanwise and chordwise planform coordinate. The Ritz method is used to obtain an approximate stationary solution to the variational condition on the energy of the wing box structure and applied loading. Upper and lower plate deflections are calculated from this "center plane" deflection, using the Kirchhoff Hypothesis. The present approach is not to relax this condition to allow crossections to be non-perpendicular to the center plane, since it would require significant changes to the program structure. Instead, both the upper and the lower plate are treated as independent plate systems (Fig. 2). Each subsystem has its own reference coordinate system and set of deflection functions. These reference coordinate systems have a vertical offset from the original coordinate system, equal to the average vertical coordinate of the plate. The plate line (center line +/- depth) of the original representation effectively becomes the new system's center line, where the depth is equal to half the plate thickness. Within each system, the Kirchhoff Hypothesis is assumed to hold, which should be fair as long as the plates are thin and have small camber. Only a minor change to the original ELAPS code was necessary for implementation of the individual reference planes; all other modifications are merely re-definition of input data.

These two (originally independent) systems are then connected by simple shear panels. As a result, the order of the dynamic system doubles when the displacement function sets are not changed from the original choice. However, changes to the code are minimal, since the shear panel kinetic and strain energies can simply be added to the values of the remaining structure.

Shear panels are assumed to be vertical and divided along their length by a specified number of equidistant points. Within each such "integration interval", this partition is divided into two triangular segments. Under the assumption that the thickness changes are small and the only connection between this incremental shear panel and the remaining structure (including other panel increments) is at its three vertices, the shear stress in it is constant and is a quadratic function of the vertex displacements. The equivalent approach is used for the panel kinetic energy/mass contribution.

Correlation of this extended equivalent plate analysis with the original ELAPS and the finite element analysis in ASTROS was performed using a sample case for a large, swept, high aspect ratio jet transport wing. Figure 3 is a sketch of the main features of this sample case. Some differences between the ELAPS and ASTROS models could not be avoided due to modeling restrictions in ELAPS. Plate and shear panel thicknesses are listed in Table 1. The models include 21 ribs (perpendicular to spars, 0.1 in. thick), which are not shown in Fig. 3. Shear web masses are included as concentrated masses in the original ELAPS input, and ASTROS "post" rods are modeled as concentrated masses in both ELAPS representations. In the "ELAPS + Shear Panels" case, the wing is rotated such that the spars are roughly parallel to the spanwise coordinate, which resulted in a reduced number of deflection functions necessary. The root is clamped in all cases; springs simulate proper support conditions for the latter case.

Tables 2 and 3 show comparisons of modal analyses obtained with the three different models. The "mode type" refers to the dominant characteristic; for example, "1B" is the first beamwise mode, "2C" the second chordwise mode, and "2T" the second torsional mode. This distinction is very difficult when certain modes are highly coupled, like the fifth and sixth mode, which contain both third beamwise bending and first torsion contributions (Fig. 4). The order of the ELAPS modes 5 and 6 are swapped to more closely resemble the ASTROS mode shapes.

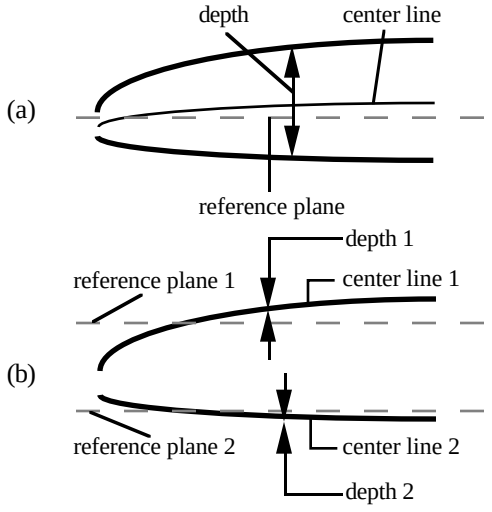

Fig. 2: Wing Box Geometry in original ELAPS (a) and for Inclusion of Shear Panels (b)

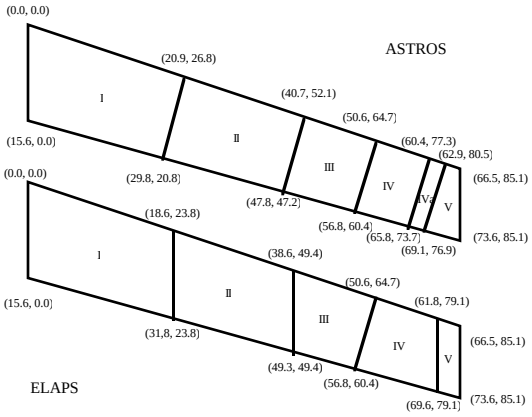

(not to scale; coordinates in ft.)

Fig. 3: ELAPS and ASTROS Representations of Sample Wing

	Plate Thickness [in]		Spar Web Thickness [in]	
Segment	ELAPS	ASTROS	ELAPS	ASTROS
I	0.300	0.300	0.200	0.200
II	0.200	0.200	0.160	0.160
III	0.125	0.125	0.120	0.120
IV	0.125	0.125	0.110	0.110
IVa	-	0.125	-	0.100
V	0.100	0.100	0.100	0.100

Table 1: Sample Wing Internal Layout

Mode Type	Baseline Values ASTROS	Deviation original ELAPS	Deviation ELAPS + Shear Panel
1B	1.0478 (1)	- 0.9% (1)	+ 5.6% (1)
1C	2.0578 (2)	- 2.7% (2)	- 4.5 % (2)
2B	3.8403 (3)	+ 1.4% (3)	+8.7 % (3)
2C	8.2908 (4)	- 1.8% (4)	- 4.6 % (4)
1T / 3B	8.4611 (5)	**+24.4%** (6)	**+8.1%** (6)
3B / 1T	8.9909 (6)	+1.7% (5)	- 1.2 % (5)
4B	15.0630 (7)	+ 7.5% (7)	+ 0.8 % (7)
2T	16.0284 (8)	**+26.9%** (8)	**+4.6%** (8)
3C	19.0497 (9)	- 1.6% (9)	- 5.5% (9)

Mode Number in Parentheses

Table 2: Natural Frequencies, [Hz]

Mode Type	Baseline Values ASTROS	Deviation original ELAPS	Deviation ELAPS + Shear Panel
1B	120.3	+ 2.1% (1)	+ 2.0% (1)
1C	228.2	+ 1.2% (2)	- 0.4% (2)
2B	95.3	+ 9.3% (3)	+ 12.7% (3)
2C	232.7	+ 11.5% (4)	+ 16.1% (4)
1T / 3B	114.1	- 35.8% (6)	- 52.6% (6)
3B / 1T	138.8	- 26.8% (5)	- 43.0% (5)
4B	68.3	+74.9% (7)	+ 206% (7)
2T	109.6	- 43.7% (8)	- 54.1% (8)
3C	248.3	- 20.3% (9)	- 37.1% (9)

Normalization: Maximum Translation per coordinate 1 ft

Table 3: Generalized Masses, [slugs-ft^2]

The most remarkable deviations are detected in the torsionally dominated modes. The inclusion of shear panels brings significant improvement in the natural frequencies of these modes. The generalized masses in Table 3 give an indication for the correlation of the mode shapes with the ASTROS baseline. The deviations are less encouraging than those of frequencies primarily due to a practical limitation in ELAPS: The maximum order of the deflection functions is eight spanwise and three chordwise, since numerical errors in the library routines increase excessively with function order and cause the program to terminate with an error. Note that the mode shapes in Fig. 3 require at least a sixth order polynomial in the normalized spanwise coordinate, y. Correlation can therefore be expected to decrease significantly starting with the sixth mode. However, for aeroelastic analysis of TR wings only the low order modes are of significance: Van Aken [15] reports a flutter frequency slightly below 5 Hz for an XV-15 type aircraft, while the natural frequencies of the first three uncoupled wing/nacelle modes can be found below 10 Hz. Hence, this limitation is not considered a severe drawback.

Hence, by including the new shear panel representation, the results were improved in modes which are relevant for tiltrotor aeroelastic analysis.

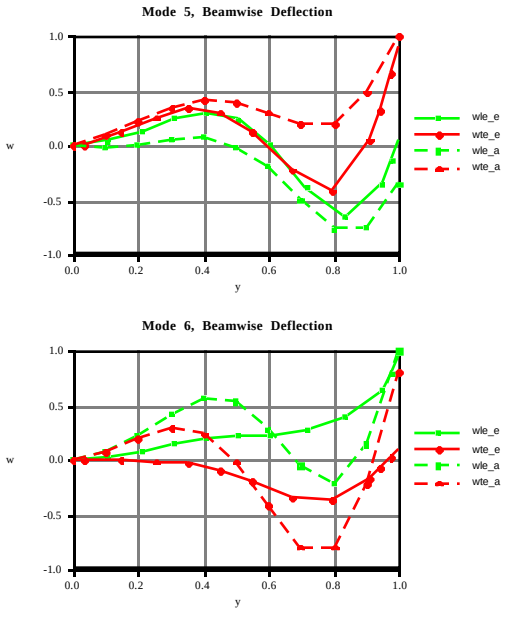

Fig. 4: "ELAPS + Shear Panels" (solid) and ASTROS (dashed) Leading and Trailing Edge (dark) Deflections

Wing Unsteady Aerodynamics

Previous studies on TR aeroelasticity have either excluded aerodynamic damping of the airframe [15], or included a quasi-steady representation [6, 16, 17]. Van Aken's results [15] translate into a reduced frequency at the stability boundary of k = 0.17, which indicates the necessity to include unsteady effects. Only Parham and Chao [18] have included a Doublet-Lattice Method in their modal analysis of the airframe, but only the modal aerodynamic damping is used in the coupled airframe-rotor stability analysis. Since these approaches did not allow a study of the effect of wing aerodynamic damping on proprotor whirl stability, a state-space unsteady aerodynamics analysis, PWAKE, based on pioneering research by Peters et al. [19], and extended by Nibbelink [20], was developed in Reference [21]. Due to an unfortunate choice of the velocity interval under investigation, the results did not allow a convincing conclusion. Furthermore, no calibration with other unsteady aerodynamic analyses was presented.

In order to allow a proper comparison of the unsteady aerodynamics only, modal information for the first six structural modes of the wing sample case described in the previous section, as obtained by the ASTROS finite element analysis, was input into PWAKE. The baseline frequency and damping values were obtained using the same structural model and ASTROS's internal Doublet-Lattice Method.

Figure 5 shows the results of a velocity sweep. PWAKE's maximum number of azimuthal harmonic shape functions, M = 13, translates into 56 unsteady aerodynamic states due to an internal numbering system. Thus, in contrast to only 6 degrees of freedom in ASTROS, the PWAKE/structure model contains 62 degrees of freedom. The plots show only those modes of the coupled model which exhibit large structural contributions (based on the length of the structural sub-partition of the eigenvectors, as compared to the wake partition). The majority of the wake-dominated modes are therefore effectively filtered out. Still, the presence of the only remaining additional mode ("f2"/"d2") complicates a comparison. At roughly 850 ft/sec it couples with the third structural mode. Below this speed, the branches match very well. Noting also that assigning labels to modes of a highly coupled system like this one is somewhat arbitrary, frequency and damping of the critical first three modes are matched satisfactorily, and the flutter speed is over-predicted by less than 5%.

Figure 6 displays frequency and damping of the coupled wing-rotor system, only slightly modified from the case in Reference [21] by introducing a wing

taper ratio of 0.8. In contrast to the previously presented results, this velocity sweep includes the stability boundary. The flutter speed with quasi-steady wing aerodynamics is only about 1.2% above that when wing aerodynamics are neglected. However, the critical mode for this particular configuration is dominated by chordwise wing bending, which shows little response to aerodynamic forces - damping of the first beamwise bending mode is much higher. This damping source could be exploited by properly tailoring the wing structure -- and in that case using quasi-steady aerodynamics is non-conservative.

The necessity of using wing unsteady aerodynamics for tiltrotor aeroelastic tailoring has been established. A new tool for this task has been developed, and correlation with the Doublet-Lattice Method was shown.

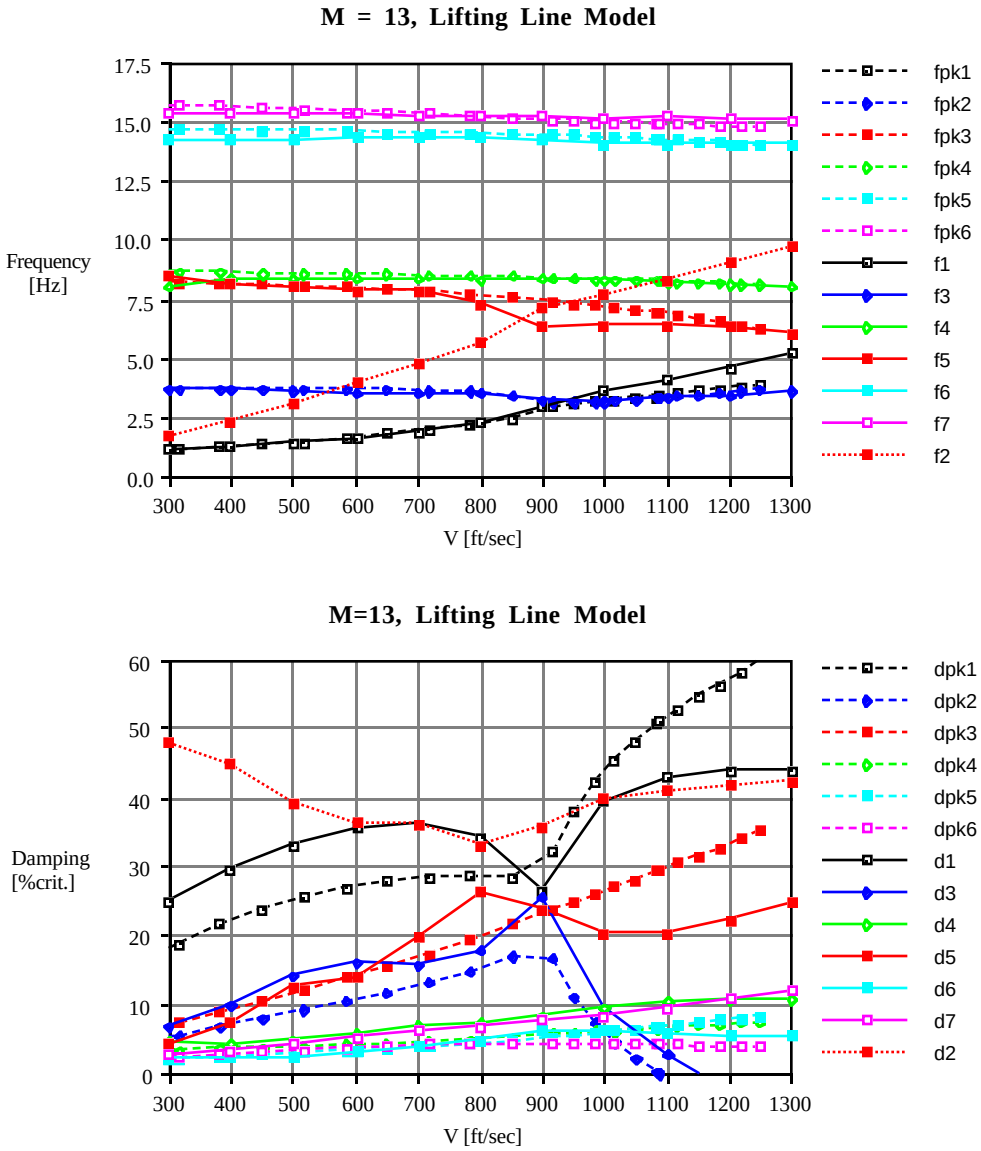

Fig. 5: Correlation of PWAKE (solid) with ASTROS Doublet Lattice Method (dashed, "pk")

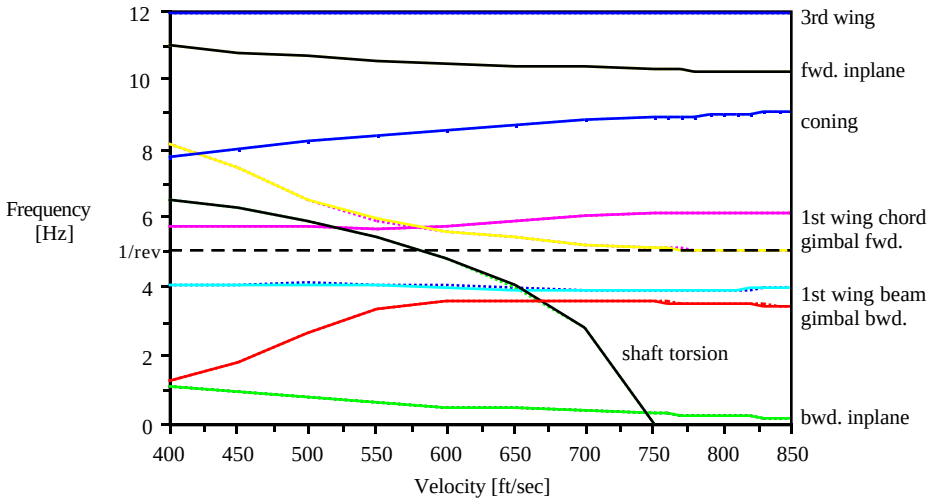

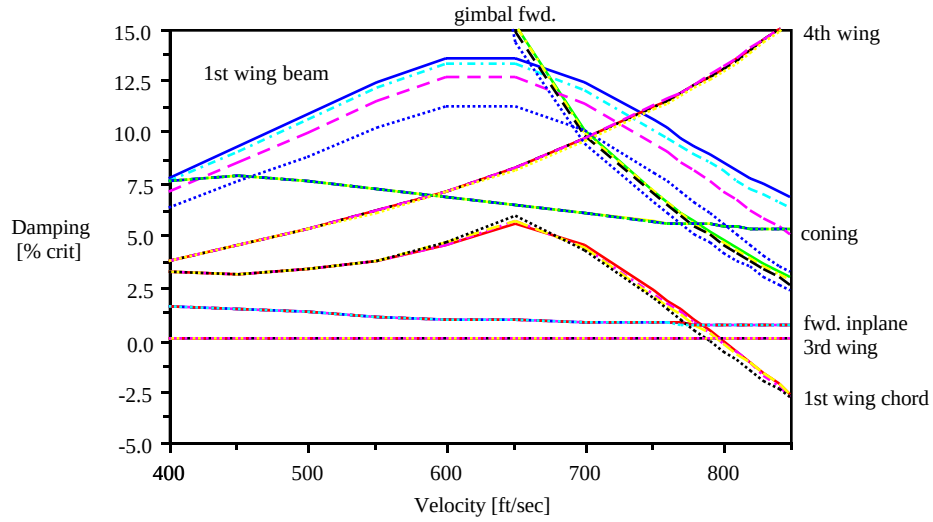

dotted lines:	no wing aerodynamics
dash-dotted lines:	unsteady aerodynamics, M = 7
dashed lines:	unsteady aerodynamics, M =15
solid lines:	quasi-steady aerodynamics

Fig. 6: Influence of Wing Aerodynamics on Wing/Rotor Stability

Rotor Aeroelasticity and Coupling of Subsystems

The Proprotor Aeroelastic Stability Analysis PASTA [3] was chosen for its simplicity and availability of the source code [8]. PASTA consists, in principle, of two parts: (1) a rigid blade rotor model with uncoupled collective and cyclic lead/lag and flapping modes; (2) a subsystem integration facility which combines rotor, elastic airframe, and rigid body modes using modal deflections at the attachment points. Modifications to both parts were made.

Early research in proprotor aeroelasticity focused on cyclic flapping modes [22] and pitch-flap coupling [23]. Nixon [6] recently pointed out the importance of cyclic lead/lag modes on proprotor stability. Collective modes have not been addressed in previous research. However, Fig. 6 (damping) shows that the flutter mode may include a large chordwise wing bending contribution, which is likely to couple kinematically into a collective flapping mode ("coning"). This mode is included in PASTA, but is decoupled from the collective lead/lag mode. CTR blade designs may feature closely spaced first elastic flapping and lead/lag modes [24]. Hence, coupling of these modes was included in PASTA by implementing a root spring system first introduced by Ormiston and Hodges [25].

Kvaternik [3] points out that rotor whirl phenomena occur at frequencies which may be close to those of the airframe in-flight rigid body modes. PASTA decouples these eigenforms from airframe elastic modes. The code has therefore be extended to include full coupling, e.g. in order to consider aerodynamic damping of fuselage pitch motions in free-free elastic modes. Furthermore, rotor longitudinal and lateral cyclic and collective pitch controls, as well as provisions for aileron and elevator deflections have been added.

The most important change was made to the subsystem coupling procedure: the original code used natural frequencies, damping coefficients, generalized masses, and real modal deflections of the airframe center of gravity and hub attachment point for a specified number of airframe modes. This is only an approximation of the aerodynamic effects, since the modal matrix of an aeroelastic system is, in general, complex. Hence, PASTA was extended to include the complete airframe/unsteady aerodynamics system and complex eigenforms. The original program was thus converted into a full representation of the "Aircraft Plant Model" of a tiltrotor, and was subsequently renamed ACP. The name also refers to the intended use of the full dynamic plant in future flutter suppression control system design, CSD. Validation of the modified analysis will commence in February.

DESIGN AND OPTIMIZATION FRAMEWORK

Overview

The size, the number of independent computational tools, and the difficulty of access to intermediate data prohibits combination of all analyses into one program. Integration of stand-alone codes using operating system level executive software bears the potential for higher flexibility and transparency. Therefore, main thrust in current research in Multidisciplinary Design Optimization is in the development and implementation of generic, fully integrated, user-friendly design environments [26,27]. These tools are still in development, and recreating a similar environment including elaborate graphical user interfaces (GUI) is beyond the scope of this research. A more promising option is to use readily available operating system utilities to link the individual programs. UNIX executive software has successfully been used in High Speed Civil Transport Optimization with the HiSAIR/Pathfinder System [28].

The present approach is very similar to this framework, but puts more emphasis on modularity, extendibility, and portability. The analytical model described above is more comprehensive than previously published studies, but by no means complete. For example, as more information on the aircraft as gathered, it may become necessary to include aerodynamic coupling of rotor and airframe in the system dynamics, investigate rotor maneuver loads, or replace PASTA's simple rotor model by a more sophisticated analysis. Adding or replacing a contributing analysis of the present approach requires reorganization of the data transfer structure, Fig. 7. If data connections between the CA's are hardwired, changing the structure requires modifying the executive software. This was avoided in the present approach, as described below.

Fig. 8 shows a schematic of the Design and Optimization Framework, DOF. The "Executive" is the central control unit. Based on whether the optimizer (DOT, [29]) requires zeroth or first order information at the current location in the design space, CAs are executed for analysis only, or in a local finite differencing loop for local sensitivities. The latter data are assembled in GSE form and solved for global sensitivities by the GSE solver. The process may be executed completely automatically, or it may pause after each optimizer step, analysis or

sensitivity evaluation, or CA run. The "Monitor" allows user interference with a running job. Job data can be checked at run time, or the process pausing schedule can be changed. All data are transferred through a central data base. The ASTROS Computer Aided Design Data Base, CADDB [30], is automatically queried using its Interactive CADDB Environment (ICE) query language, CQL. This scripting process has a longer access time, but allows maximum portability: CQL is based on the ANSI Standard for Database Languages (SQL X3.135-1986), and its special features have not been used. Hence, any other database management system (DBMS) could be used as well.

The key feature regarding flexibility and extendibility is the structure of the central data base. All design variables and behavior variables (data transfered between CAs and other relevant analysis outputs) are stored here. In addition to the current values and the variable history from previous optimization steps, the data base contains also information on where the variable is generated, and in which CAs it is needed as input. This information is located in one relational entity; thus, a change in the data flow structure results only in changes in this one entity. In other words, the data flow structure is an inherent element of the data base, not the executive software. It is readily available to the GSE solver for assembly of the GSE. It is also used to extract CA input data from the data base.

The I/O Filters play a central role in linking a CA with DOF. The input and output files of each analysis tool have in general a unique format. The filters are therefore as unique to each CA as these formats. Their task is first to extract relevant data from the output file and provide them to DOF in a standard format, second to convert input data in this standard format into a proper CA input file. Introducing a new analysis tool therefore requires supplying a new I/O filter. In order to make this task easier, the package includes utilities for updating specific data in formatted and namelist input files.

The framework is designed to allow the user as much freedom as possible in scheduling the design/optimization task. "Scheduling" refers to

(1) parallel execution of CAs;
(2) grouping of CAs into "Circuits" for analysis;
(3) grouping of CAs into "Sequences" for sensitivity calculation.

Parallel execution is possible if more than one host computer is connected to the same file server. The names of the available host computers are stored in the database, and the Executive decides on which host a CA job will be run. To date, only one CA analysis or sensitivity analysis job per computer is allowed; currently, the executive is changed to find a host computer based on the least work load.

The term "Circuit" stems from Rogers's Design Manager's Aide for Intelligent Decomposition, DeMAID [31]. A Circuit is a closely coupled feedback loop in the analysis process. Refering to Fig. 7, note that connections between the CA blocks above the main diagonal denote a data feed-forward, and below it feedback. One detects one iteration loop involving VASCOMP (output: geometry and weights as a function of e.g. wing structural weight) and ELAPS (output: wing structural weight as a function of geometry). Combining these two CAs into one Circuit results into a structure which allows sequential execution of circuits without iteration outside those Circuits (Fig. 9). Within a circuit, the CA's are executed in parallel (if enough host computers are available), until the outputs converge. If convergence is fast and/or user time is an issue, the user may chose to include all CAs in the iteration loop in order to avoid a string of parallel CA runs. If convergence is slow and/or added CPU time on the host computers is critical, breaking the analysis in the smallest Circuits possible could be advantageous. Grouping of CAs into Circuits is therefore a user database input.

A "Sequence" is a group of CAs in a local finite differencing loop. The GSE approach allows local sensitivity analyses to be performed about each CA. This may not be a good choice if the number of behavior variables is large. Consider the example from Fig. 7. Let the dynamic model include five airframe, three significant unsteady aerodynamic, and six rotor modes, so the complete system has fourteen degrees of freedom. With four control inputs (three rotor, one aileron) and output of accelerations in two points of the structure (rotor hub and aircraft center of gravity), the first order dynamic system representation has 1120 elements in its four matrices. As a result, CSD must be executed 1120 times in the local sensitivity analysis - ELAPS runs 16 times, PWAKE 176 times, and ACP 214 times, not including sensitivies with respect to design variables!

Based on computational effort involved, the user may decide to group CAs instead. Fig. 10 shows an example where ELAPS, PWAKE, ACP, and CSD form the Sequence "Dynamics". Since Fig. 7 indicates no iteration among these CAs, each CA is executed only 18 times. The user is free to decide between the first option - accuracy and transparency - and the second option - computational effort - or any intermediate grouping by specifying the Sequence grouping as a database entry. This option is currently being implemented.

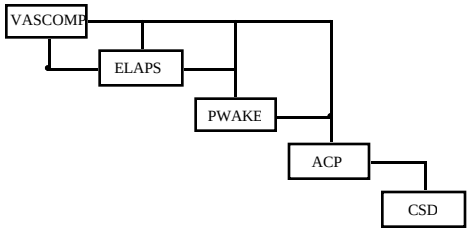

Fig. 7: Data Transfer Structure - N^2 Diagram

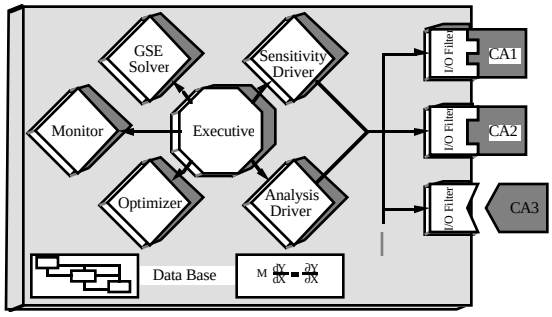

Fig. 8: Design and Optimization Framework Schematic

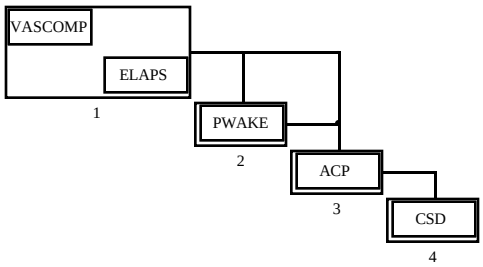

Fig. 9: Circuits

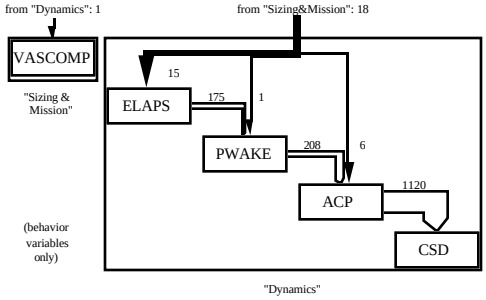

(numbers indicate behavior variable inputs)

Fig. 10: Sequences

Sample Case

For validation of DOF, a slightly modified design problem for a Boeing 727 type aircraft [31] was used. All analyses are based on simple equations, which have been grouped into four Contributing Analyses (see Appendix). A fifth CA is added for calculation of the PI as an objective function, and proper formulation of upper constraints on take-off and landing field length and wing aspect ratio, and lower constraints on achievable climb gradients, fuel balance, and useful load fraction. Wing span, fuselage length, wing area, installed thrust, and take-off gross weight are used as design variables. In total, the problem is described by 22 behavior variables, which include six constraints and the objective function. Fig. 11 indicates two closely coupled iteration loops. D, A, and W are combined into one Circuit. The CAs are not grouped into sequences of more than one CA.

Since the CAs are represented by simple analytical expressions, CA input-output sensitivities can be directly obtained without finite differencing. The CA equations and analytical sensitivities were first hard-coded in a FORTRAN program (Method 1) which allows global sensitivity calculation by either global finite differencing or solution of the GSE (local sensitivity analysis using analytical sensitivities). Then the CAs were programmed as little stand-alone codes, and coupled with the DOF (Method 2). Optimization runs with the framework itilized either global or local finite differencing (GSE approach). Objective function and design variable histories for global finite differencing and GSE approach are shown in Figures 12 and 13, respectively. All data are normalized by their values at iteration 0. The initial design violates the fuel weight ratio constraint by roughly 6% (i.e. fuel weight required is 106% of fuel weight available).

If global finite differencing is used to obtain objective function and constraint first order information (Fig. 12), the results differ significantly. Note in particular the objective function "dip" at the first iteration and subsequent oscillations of the fuselage length, l, when using Method 1. There is no indication that both methods might converge to a similar solution. The GSE approach shows much

better correlation (Fig. 13). With Method 1, the fuselage length still fluctuates significantly, but appears to converge towards the value from Method 2. The objective function history supports the impression that with stricter convergence criterion both methods will produce very similar results. This design is very similar to that produced by Method 1 with global finite differencing.

The are two explanations for the deviations between GSE and global finite differencing results with Method 2 (DOF). First, rounding errors are likely to occur as a result of data filtering and conversion. Second, each global finite differencing step is equivalent to a complete analysis cycle, including iteration. Although the convergence limits are the same for Methods 1 and 2, there is still a potential for error accumulation. The GSE approach does not require iteration, and is hence more robust with respect to accumulated errors.

Investigation of the behavior of the fuselage length allows another statement about the GSE approach. This design variable has a weak influence on the objective function through the fuselage drag coefficient (see Appendix, "Zero Lift Drag"). The function is nonlinear since it contains a logarithm. If global finite differencing is used, this nonlinearity is hidden in the analysis loop. Fuselage drag might be termed a highly sensitive state which is barely observable through the system output (objective function, constraints), in analogy to controls terminology. Local finite differencing measures the sensitivity of this state more directly; it appears that this increases "observability" and improves convergence behavior.

Experience with this sample case led to the conclusion that using the GSE approach is more robust to rounding errors and improves overall convergence behavior through improved observability of behavior variable responses.

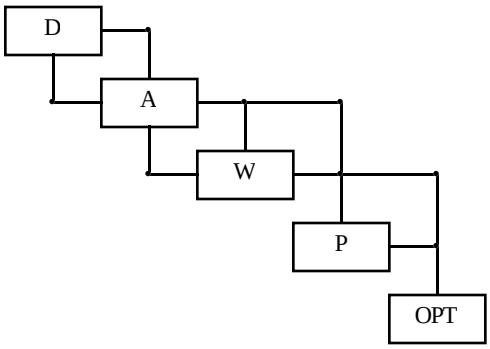

Fig. 11: Sample Case N^2 Diagram

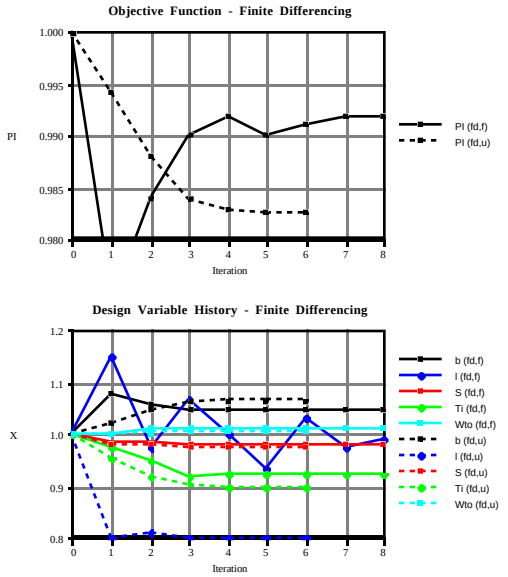

solid: Method 1 - FORTRAN hard-coded;
dashed: Method 2 - UNIX DOF Framework

Fig. 12: Optimization History, Global Finite Differencing

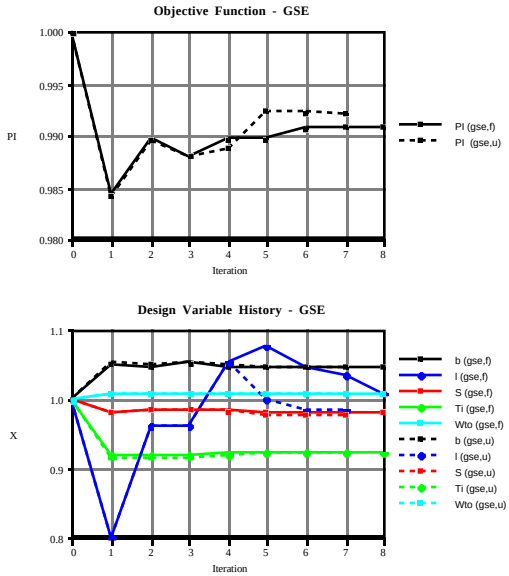

solid: Method 1 - FORTRAN hard-coded;
dashed: Method 2 - UNIX DOF Framework

Fig. 13: Optimization History, GSE

CONCLUDING REMARKS

Preliminary results support the necessity of all code updates as well as the comprehensiveness of the approach. The scope of the task demanded extensive research in Multidisciplinary Design Optimization (MDO). The Design and Optimization Framework, DOF, developed as a result of these considerations, has proven to be a useful utility for optimization of general, coupled, complex systems. With the exception of control system design (CSD), all Contributing Analysis tools have been updated. VASCOMP is connected to DOF; ELAPS and PWAKE have been validated. DOF itself has been completed. Based on this status, exploration of the CTR design space will commence in early 1995.

APPENDIX

Sample Case Contributing Analyses

Zero Lift Drag D

zero lift drag coefficient

$$c_{D0} = (c_{D0})_{wing} + (c_{D0})_{body} + \Delta c_{D0}$$

wing contribution

$$(c_{D0})_{wing} = 1.1 c_{f,wing}\left(1 + 1.2\left(\tfrac{t}{c}\right) + 100\left(\tfrac{t}{c}\right)^4\right)\overline{S}_{wet}$$

body contribution

$$(c_{D0})_{body} = c_{f,body}\left(1 + 0.0025\left(\tfrac{l}{d}\right) + 60\Big/\left(\tfrac{l}{d}\right)^3\right)\overline{S}_S$$

increment drag coefficient

$$\Delta c_{D0} = 0.005$$

body wetted surface ratio

$$\overline{S}_S = \pi\frac{dl}{S}\left(1 - 2\tfrac{d}{l}\right)^{2/3}\left(1 + \left(\tfrac{d}{l}\right)^2\right)$$

wing wetted surface ratio

$$\overline{S}_{wet} = 2$$

fuselage diameter

$$d = 1.83\left(4.325\frac{N_P}{l} + 1\right)$$

skin friction coefficient

$$c_f = 0.455\left(\log_{10}\left(\frac{Vl_{ref}}{\nu}\right)\right)^{-2.58}$$

Body: $l_{ref} = l$; Wing: $l_{ref} = c$;
wing chord, c= S/b

Aerodynamic Performance A

lift-to-drag ratio

$$\frac{L}{D} = \frac{c_L}{c_{D0} + kc_L{}^2}$$

optimum L/D for cruise

$$\left.\frac{L}{D}\right|_{opt} = \frac{1}{2}\frac{1}{\sqrt{c_{D0}k}}$$

speed for best range (cruise)

$$V_{BR} = \sqrt{\frac{2W_{TO}}{\rho S\sqrt{\frac{c_{D0}}{k}}}}$$

lift coefficient

$$c_L = \frac{2W_{TO}}{\rho V^2 S}$$

quadratic drag polar

$$k = \frac{1}{\pi Ae}$$

Oswald Efficiency Factor

$$e = 0.96\left(1 - \left(\tfrac{d}{b}\right)^2\right)$$

wing aspect ratio
$A = b^2/S$

Weights W

fuel weight ratio available

$$R_{fa} = 1 - \frac{W_{pay}}{W_{TO}} - \frac{W_{fix}}{W_{TO}} - \frac{W_{empty}}{W_{TO}}$$

empty weight ratio

$$\frac{W_{empty}}{W_{TO}} = \frac{0.9592}{W_{TO}{}^{0.0638}} + 0.38\frac{T_i{}^{0.9881}}{W_{TO}}$$

fuel weight ratio required for mission

$$R_{fr} = 1.1\left(1 - 0.95\frac{W_f}{W_i}\right)$$

ratio of take-off weight to landing weight

$$\frac{W_f}{W_i} = \exp\left(-\frac{Rb_t}{V_{cruise}\left.\frac{L}{D}\right|_{cruise}}\right)$$

useful load fraction

$$\overline{U} = \frac{W_{pay}}{W_{TO}} + R_{fr}$$

Performance P

landing field length

$$S_L = 118\frac{\left(W_{TO}/[lb]\right)}{\left(S/[ft^2]\right)c_{L\max}} + 400$$

take-off field length

$$S_{TO} = 20.9\frac{\left(W_{TO}/[lb]\right)}{\left(S/[ft^2]\right)c_{L\max}}\frac{W_{TO}}{T_i} + 87\sqrt{\frac{\left(W_{TO}/[lb]\right)}{\left(S/[ft^2]\right)c_{L\max}}}$$

achievable climb gradient, landing, OEI

$$q_L = \frac{T_i}{W_{TO}}\frac{N-1}{N} - \left(\frac{L}{D}\right)^{-1}\Bigg|_{L/TO}$$

achievable climb gradient, take-off, OEI

$$q_{TO} = \frac{T_i}{W_{TO}}\frac{N-1}{N} - \left(\frac{L}{D}\right)^{-1}\Bigg|_{L/TO}$$

mission fuel weight balance

$$\overline{R}_f = \frac{R_{fa}}{R_{fr}}$$

REFERENCES

[1] Wilkerson, J. B., and Taylor, R. S., "Civil Tiltrotor Aircraft: A Comparison of Five Candidate Designs," presented at the 44th Annual Forum of the American Helicopter Society, Washington, DC, June 1988.

[2] Sobieszczanski-Sobieski, J., "Sensitivity of Complex, Internally Coupled Systems," *AIAA Journal*, Vol. 28, No. 1, January 1990.

[3] Kvaternik, R. G., "Studies in Tiltrotor VTOL Aircraft Aeroelasticity," PhD Dissertation, Department of Solid Mechanics, Case Western Reserve, June 1973.

[4] Schleicher, D. R., Phillips, J. D., and Carbajal, K. B., "Design Opimization of High-Speed Proprotor Aircraft," NASA-TM-103988, April 1993.

[5] Schoen, A. H., Rosenstein, H., Stanzione, K., and Wisniewski, J. S., "User's Manual for VASCOMP II, The V/STOL Aircraft Sizing and Performance Computer Program," Boeing Vertol Company Report D8-0375, Vol. VI, Third Revision, May 1980.

[6] Nixon, M. W., "Parametric Studies for Tiltrotor Aeroelastic Stability in High-Speed Flight," 33rd AIAA/ASME/ASCE/AHS Structures, Structural Dynamics, and Materials Conference, Dallas, Texas, April 1992.

[7] Stettner, M., and Schrage, D. P., "Tiltrotor Performance Sensitivities for Multidisciplinary Wing Optimization," American Helicopter Society International Specialists Meeting on Rotorcraft Multidisciplinary Design Optimization, Atlanta, GA, April 1993.

[8] Stettner, M., and Schrage, D. P., "An Approach to Tiltrotor Wing Aeroservoelastic Optimization through Increased Productivity," 4th AIAA/ USAF/NASA/OAI Symposium on Multidisciplinary Analysis and Optimization, Cleveland, Ohio, September 1992.

[9] Giles, G. L., "Further Generalizations of an Equivalent Plate Analysis for Aircraft Structural Analysis," *Journal of the Aircraft*, Vol. 26, No. 1, January 1989.

[10] Friehmelt, H., "Design of a Tiltrotor Wing for a EUROFAR-type Configuration," Diploma Thesis, Technische Universität Braunschweig/ Georgia Institute of Technology, March 1993.

[11] Studebaker, K., and Matuska, D., "Variable Diameter Tiltrotor Wind Tunnel Test Results," presented at the 49th Annual Forum of the American Helicopter Society, St. Louis, Missouri, May 1993.

[12] Whetstone, W. D., "EISI-EAL Engineering Anaysis Language Reference Manual - EISI-EAL System Level 2091," Engineering Information Systems Inc., San Jose, California, July 1983.

[13] Livne, E., Sels, R. A., and Bhatia, K. G., "Lessons from Application of Equivalent Plate Structural Modeling to an HSCT Wing," 34th AIAA/ASME/ASCE/AHS Structures, Structural Dynamics, and Materials Conference, La Jolla, California, April 1993.

[14] Johnson, E. H., and Venkayya, V. B., "Automated Structural Optimizations System (ASTROS)," AFWAL-TR-88-3028, Flight Dynamics Directorate, Wright Laboratory, Air Force Systems Command, Wright-Patterson Air Force Base, Ohio, December 1988.

[15] van Aken, J. M., "Alleviation of Whirl-Flutter on Tiltrotor Aircraft using Active Controls," 47th Annual Forum of the American Helicopter Society, Phoenix, Arizona, May 1991.

[16] Frick, J., and Johnson, W., "Optimal Control Theory Investigation of Proprotor/Wing Response to Vertical Gust," NASA-TM-X-62384, September 1974.

[17] Nasu, K., "Tilt-Rotor Flutter Control in Cruise Flight," NASA - TM - 88315, December 1986.

[18] Parham, T. C., and Chao, D., "Tiltrotor Aeroservoelastic Design Methodology at BHTI," 45th Annual Forum of the American Helicopter Society, Boston, Massachusettes, May 1989.

[19] Peters, D. A., Boyd, D. B., and He, C. J., "Finite-State Induced Flow Model for Rotors in Hover and Forward Flight," *Journal of the American Helicopter Society*, Vol. 34, No. 4, October 1989.

[20] Nibbelink, B. D., and Peters, D. A., "Flutter Calculations for Fixed and Rotating Wings with State-Space Inflow Dynamics," 34th AIAA / ASME / ASCE / AHS / ASC Structures, Structural Dynamics, and Materials Conference, La Jolla, California, April 1992

[21] Stettner, M., Peters, D. A., and Schrage, D. P., "Application of a State-Space Wake Model to Tiltrotor Unsteady Aerodynamics," American Helicopter Society Aeromechanics Specialists Meeting, San Francisco, CA, January 1994.

[22] Wernicke, K. G., and Gaffey, T. M., "Review and Discussion of 'The Influence of Blade Flapping Restraint on the Dynamic Stability of Low Disk Loading Propeller-Rotors," 23rd American Helicopter Society Annual Forum, Washington, D.C., May 1967.

[23] Gaffey, T. M., "The Effect of Positive Pitch-flap Coupling (negative δ_3) on Rotor Blade Motion Stability and Flapping," *Journal of the American Helicopter Society*, Vol. 14, No. 2, 1969.

[24] Caramaschi, V., and Maffioli, G., "Design and Manufacturing Concepts of Eurofar Model#2 Blades," 48th American Helicopter Society Annual Forum, Washington, D.C., June 1992.

[25] Ormiston, R. A., and Hodges, D. H., "Linear Flap-Lag Dynamics of Hingeless Helicopter Rotor Blades in Hover," *Journal of the American Helicopter Society*, Vol. 17, No. 2, 1972.

[26] Townsend, J. C., and Weston, R. P., "An Overview of the Framework for Interdisciplinary Design Optimization (FIDO) Project," NASA-TM-109058, July 1994.

[27] Hale, M. A., and Craig, J.I ., "Preliminary Development of Agent Technologies for a Design Integration Framework, 5th AIAA/ USAF/NASA/OAI Symposium on Multidisciplinary Analysis and Optimization, Panama City, Florida, September 1994.

[28] Jones, K. H., Randall, D. P., and Cronin, C. K., "Information Management for a Large Multdisciplinary Project," 4th AIAA/ USAF / NASA / OAI Symposium on Multidisciplinary Analysis and Optimization, Cleveland, Ohio, September 1992.

[29] Anonymous, "DOT Users Manual," Version 4.00, Vanderplaats, Miura & Associates, Inc., Goleta, California, April 1993.

[30] Herendsen, D. L., and Ludwig, M. R., "Interactive Computer Aided Desgin Database (CADDB) Environment User's Manual," AFWAL-TR-88-3060, Flight Dynamics Directorate, Wright Laboratory, Air Force Systems Command, Wright-Patterson Air Force Base, Ohio, December 1988.

[31] Rogers, J., "A Knowledge-Based Tool for Multilevel Decomposition of a Complex Design Problem," NASA-TP-2903, May 1989.

[32] Mistree, F., Marinopoulos, S., Jackson, D. M., and Shupe, J. A., "The Design of Aircraft Using the Decision Support Problem Technique," NASA-CR-4134, April 1988.